

SSR ANALYSIS WITH A NEW ANALYTIC MODEL OF THYRISTOR CONTROLLED SERIES CAPACITOR

G.N.Pillai

Indian Institute of Technology
Roorkee, India

D. Jovcic

Kings College, University of Aberdeen
Aberdeen, Scotland

Abstract - This paper presents the use of new model of a Thyristor Controlled Series Capacitor (TCSC) in studies of subsynchronous resonance (SSR). The new analytical model is developed by using frequency response of the non-linear TCSC segment to derive a simplified non-linear state space model, where the frequency of the dominant TCSC complex poles shows linear dependence on the firing angle. The non-linear TCSC model is linearised and linked with the generator-shaft system model and the controller model that also includes a Phase Locked Loop model. The test system selected for the study is the IEEE first benchmark model for SSR studies. The SSR analysis is studied through eigenvalues analysis using MATLAB and the results are validated through PSCAD/EMTDC simulation studies.

Keywords: modeling, subsynchronous resonance, eigenvalue analysis, thyristor-controlled series capacitor, flexible ac transmission system

1 INTRODUCTION

Thyristor Controlled Series Capacitor (TCSC) is a series FACTS device which allows rapid and continuous changes of the transmission line impedance. It has great application potential in accurately regulating the power flow on a transmission line, damping inter-area power oscillations, mitigating subsynchronous resonance (SSR) and improving transient stability.

The characteristics of a TCSC at steady-state and very low frequencies can be studied using fundamental frequency analytical models [1],[2]. These particular models recognize the importance of having different approach from SVC modeling (assuming only line current as a constant) which, although more demanding on the derivation, gives the most accurate TCSC model.

The fundamental frequency models are inadequate for the study of SSR since they only give the relationship among fundamental components of variables when at steady-state. Conventionally, the electromagnetic transient programs like EMTP or PSCAD/EMTDC are used for TCSC transient stability analysis and SSR studies with systems containing TCSC. These simulation tools are accurate but they employ trial and error type studies only, implying use of a large number of repetitive simulation runs for varying parameters in the case of complex analysis or design tasks. On the other hand, the application of dynamic systems analysis techniques

or modern control design theories would bring benefits like shorter design time, optimization of resources and development of new improved designs. In particular, the eigenvalue and frequency domain analysis are widely recognized tools and they would prove invaluable for system designers and operators. These techniques however always necessitate a suitable and accurate dynamic system model.

The analytical approach to study SSR with the sampled-data models of TCSC [3-4] can become cumbersome and impractical for large power systems because of the requirement for a sampled-data model of the full system. The modeling principle reported in [5] avoids discretisation and stresses the need for assuming only line current as an ideal *sine*, however it employs rotating vectors that might be difficult to use with stability studies, and only considers the open loop configuration. The model in [5] is also oversimplified because of the use of equivalent reactance and equivalent capacitance that might be deficient when used in wider frequency range. Most of these reported models are therefore concerned with a particular system or particular type of study, use overly simplified approach and do not include control elements or Phase Locked Loops (PLL).

In this study we present a suitable linear continuous TCSC model and use it to study the small signal torsional dynamics of a TCSC compensated power system. This model has reasonable accuracy for the dynamic studies in the sub-synchronous frequency range and it incorporates common control elements including PLL. To enable flexibility of the model use with different AC systems and shaft system, the model structure adopts interlinked subsystem units in similar manner as with SVC modeling in [6]. The interactions between network and the generator are studied on the IEEE SSR Benchmark system [7] which has purposely adjusted parameters to enable very weak damping of the subsynchronous modes. The validation of the eigenvalues analysis is achieved using PSCAD/EMTDC simulation.

2 TEST SYSTEM

The test system for the study is a long transmission system compensated by a TCSC and connected to a firm voltage source on each side. Figure 1 shows a single line diagram of the test system where the transmission line is represented by a lumped resistance and inductance in accordance with the approach for sub-synchronous resonance studies [7]. Each phase of the TCSC is com-

posed of a fixed capacitor in parallel with a Thyristor Controlled Reactor (TCR). The TCSC is controlled by varying the phase delay of the thyristor firing pulses synchronized through a PLL to the line current waveform. The controller is of a PI type with a feedback filter and a series compensator.

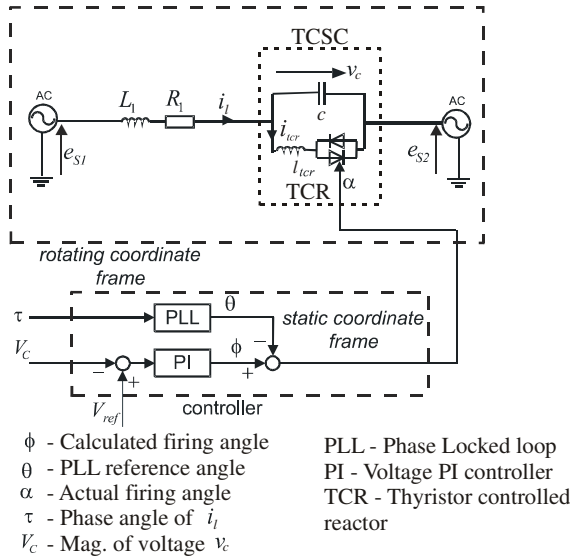


Figure 1: Test system configuration.

3 NON-LINEAR TCSC DYNAMICS

The voltage across the TCSC capacitor (v_c) comprises an uncontrolled and a controlled component, and it is presumed that the line current is constant over one fundamental cycle in accordance with [1-5]. The uncontrolled component v_1 , is a *sine* wave (unaffected by thyristor switchings) and it is also constant over a fundamental cycle since it is directly related to the amplitude of the prevailing line current. The controlled component v_2 is a non-linear variable that depends on circuit variables and on the TCR firing angle.

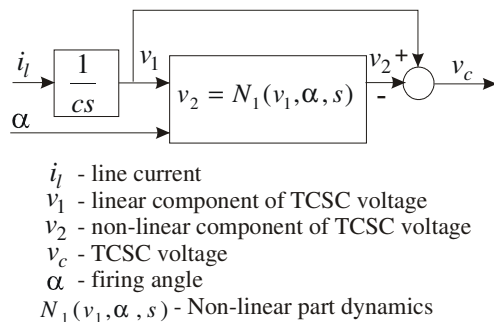


Figure 2: TCSC model structure.

In this study, the controlled component is represented as a non-linear function of the uncontrolled component and firing angle, $v_2 = N_1(v_1, \alpha, s)$, as shown in Figure 2. With this approach, $N_1(v_1, \alpha, s)$ captures the non-linear

phenomena caused by thyristor switching influence and all internal interactions with capacitor voltage assuming only that the line current and v_1 are linear. We seek in our work to study dynamics of $N_1(v_1, \alpha, s)$ in a wider frequency range and also to offer a simplified representation for fundamental frequency studies.

The fundamental components of reactor current i_{tcr} and the voltages v_1 and v_2 are selected as state variables and the non-linear state-space model is presented as:

$$sv_1 = \frac{1}{c} i_l \quad (1)$$

$$sv_2 = g \frac{1}{c} i_{tcr} \quad (2)$$

$$s i_{tcr} = g \frac{1}{l_{tcr}} v_1 - g \frac{1}{l_{tcr}} v_2 \quad (3)$$

$$v_c = v_1 - v_2 \quad (4)$$

where g represents the switching function: $g=1$ for thyristor in conduction, and $g=0$ for thyristor in blocking state.

The goal of the dynamic modeling is to derive a dynamic expression for $N_1(v_1, \alpha, s)$ of satisfactory accuracy in the sub-synchronous frequency range and for small signals around the steady-state operating point. The frequency response of TCSC is studied assuming that the input voltage is:

$$v_1 = A_0 \sin(2\pi f_o t) + A_{inj} \sin(2\pi f_{inj} t) \quad (5)$$

where the first *sine* signal denotes the steady-state operation with all parameters constant. The second term is the input in the experimental frequency response and it has small magnitude $A_{inj} \ll A_0$. The injection frequency is varied in the range ($f_{inj} \in 1, 150 \text{ Hz}$). The output v_2 is monitored and the first harmonic of the Fourier series (same frequency as f_{inj}) is compared with the input signal to obtain the frequency response.

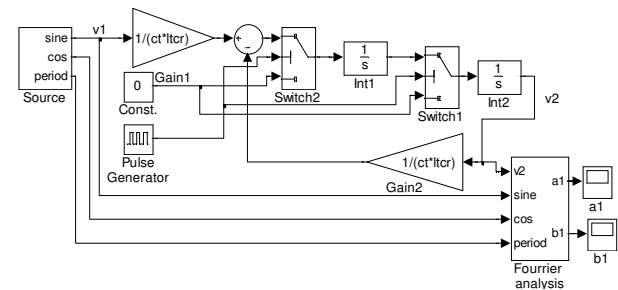


Figure 3: Experimental frequency response set-up with the SIMULINK model for the non-linear TCSC segment.

The non-linear segment of the model (2)-(3) is simulated in SIMULINK environment as shown in Figure 3. The source generates a *sine* signal with the above range of frequencies f_{inj} and for each frequency the

magnitude and phase of the first harmonic of the output voltage v_2 is observed.

The pulse generator produces equally spaced conduction intervals that are based on the fundamental frequency period and which are dependent on the firing angle. It is presumed that the fundamental frequency components are unaffected by the injection signal, and therefore the firing pulses are equally spaced.

The experimental frequency response over the range of frequencies is repeated for all values of the firing angle $\alpha \in (0, 90^\circ)$ with a one-degree increment. For each firing angle, the gain and phase values across the frequency range are plotted and Figure 4 shows an example for the particular firing angle $\alpha = 76^\circ$. Observing the frequency response curves in Figure 4 and others for other firing angles, it is concluded that the system shows higher order properties and it becomes clear that it has dominant second order dynamics. The following transfer function is proposed:

$$\frac{v_2(s)}{v_1(s)} = \frac{\frac{s^2}{w_n^2} + \frac{2\zeta_n s}{w_n} + 1}{\frac{s^2}{w_d^2} + \frac{2\zeta_d s}{w_d} + 1} \quad (6)$$

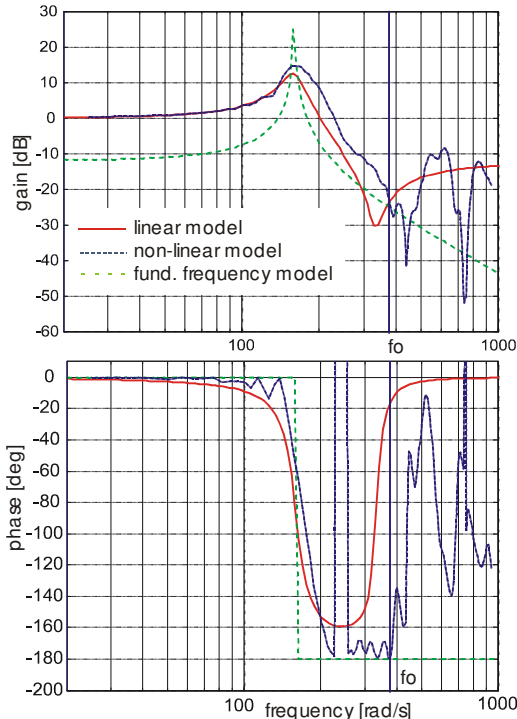


Figure 4: Frequency response for the non-linear TCSC segment. Test system 1 with the firing angle $\alpha = 76^\circ$.

The modeling task is to determine the four parameters in the above expression (ω_b , ω_n , ζ_n and ζ_d) to enable adequate model accuracy.

The characteristic peak in the gain frequency response is caused by the dominant complex poles and

each of the troughs by a pair of complex zeros. By monitoring the location of the peak in the frequency response across the range of firing angle values and the circuit parameters, the graph of ω_b versus firing angle is derived as shown in Figure 5.

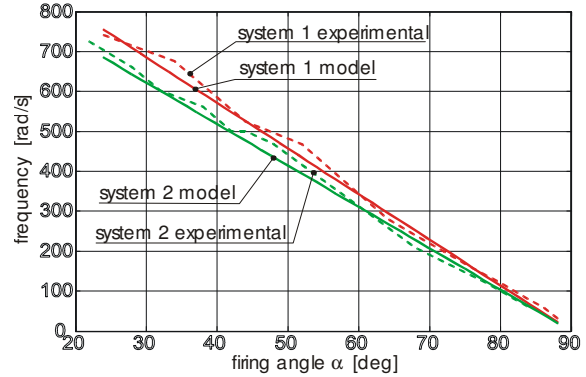


Figure 5: Linear relationship between the denominator characteristic frequency (ω_b) and the firing angle α . (System 1 has 75% compensation and System 2 has 40% compensation)

It is concluded that the denominator characteristic frequency ω_b is a linear function of the firing angle where the actual mathematical formula can be readily derived as given below in (7). The linear formula shows very good accuracy and it reflects well the variation in circuit parameters as seen in Figure 5. Analysing (7) it is seen that the resonant frequency of a TCSC starts at the natural resonance of L-C circuit (for $\alpha = 0$) and it linearly reduces with the increase in the firing angle. The formula has importance for the practical design since it points to the TCSC firing angles that should be avoided if the connected system is sensitive to resonance in a particular frequency range (SSR problems for example).

The remaining unknowns in (6) are determined in a similar manner, by matching the frequency response and the final step responses, and the proposed final formulae are given below.

$$w_d = \frac{\pi - 2\alpha}{\pi \sqrt{l_{TCR} c}} \quad (7)$$

$$\zeta_d = 0.38 \cos(\alpha) \quad (8)$$

$$w_n = \frac{\pi f_o 10^{-3}}{\sqrt{l_{TCR} c}} \left(1.7 + \sqrt{10} \frac{\alpha}{\tan^4(\alpha)} \right) \quad (9)$$

$$\zeta_n = 0.2 \cos(\alpha) \quad (10)$$

The simulated frequency response with the above transfer function is shown in Figure 4 where satisfactory matching is observed compared to PSCAD/EMTDC nonlinear simulation, except at higher frequencies. It is emphasized here that the model zeros fall in higher frequency region, implying influence of sampling sys-

tem phenomena, and the numerator parameters in (6) are open for further research and improvements.

4 SMALL-SIGNAL TORSIONAL OSCILLATIONS STUDIES

We shall now demonstrate the validity of the TCSC model in small signal torsional oscillation studies. The IEEE first benchmark model (FBM) contains a generator system, a shaft system and the compensated transmission system. The linearized models of these subsystems are first derived and then they are added together for eigenvalue analysis.

4.1 Combined Generator and Shaft system model

The linearized generator electrical and mechanical equations for the IEEE-first benchmark model are derived in the same manner as given in [8]. The linearized state equations are given by

$$\Delta \dot{x}_G = [A_G] \Delta x_G + [B_G] \Delta u_G \quad (11)$$

$$\Delta y_G = [C_G] \Delta x_G \quad (12)$$

where the state vector and the vectors Δu_G and Δy_G output vector are given respectively by

$$x_G^T = [\psi_d \quad \psi_q \quad E'_d \quad E'_q \quad \delta_g \quad S_e \quad T_{g,e} \quad S_g \quad T_{LPB,g} \quad S_{LPB} \quad T_{LPA,LPB} \quad S_{LPA} \quad T_{IP,LPA} \quad S_{IP} \quad T_{HP,IP} \quad S_{HP}]$$

$$u_G^T = [v_D \quad v_Q] \text{ and } y_G^T = [i_{LD} \quad i_{LQ}]$$

In the above equation ψ denotes the stator flux linkage, E^t denotes the transient internal voltage, δ_g is the rotor angle, S denotes the per unit slip and T denotes the torque. Note that the six mass mechanical system contains the generator (g), exciter (e), LPB, LPA, IP and HP turbine shafts. The torques between these shafts are indicated by subscripts. The vector Δu_G contains the terminal voltages and the vector Δy_G contains the armature currents.

4.2 TCSC model

The model (6) is transferred to the state space domain as given below:

$$\begin{aligned} s x_1 &= i_1 / c \\ s x_2 &= a_{ic23} x_3 \\ s x_3 &= a_{ic31}(\alpha) x_1 + a_{ic32}(\alpha) x_2 + a_{ic33}(\alpha) x_3 \\ s x_4 &= a_{ic41}(\alpha) x_1 + a_{ic42}(\alpha) x_2 + a_{ic43}(\alpha) x_3 + a_{ic44} x_4 \\ v_c &= x_4 \end{aligned} \quad (13)$$

where the parameters are:

$$\begin{aligned} a_{ic23} &= 1 \\ a_{ic31}(\alpha) &= \omega_d^2 \quad a_{ic32}(\alpha) = -\omega_d^2 \quad a_{ic33}(\alpha) = -\omega_d \zeta_d \\ a_{ic41}(\alpha) &= \frac{1}{T_f} \left(1 - \frac{\omega_d^2}{\omega_n^2} \right) \quad a_{ic42}(\alpha) = \frac{1}{T_f} \left(\frac{\omega_d}{\omega_n^2} - 1 \right) \\ a_{ic43}(\alpha) &= \frac{1}{T_f} \left(\frac{\zeta_d \omega_d}{\omega_n^2} - \frac{\zeta_n}{\omega_n} \right) \quad a_{ic44} = \frac{1}{T_f} \end{aligned} \quad (14)$$

and the states are defined as:

$$x_1 = v_1, \quad x_2 = v_1 \left(\frac{1}{\omega_d^2} s^2 + \frac{\zeta_d}{\omega_d^2} s + 1 \right) \quad (15)$$

$$x_3 = s x_2, \quad x_4 = \frac{v_1 - v_2}{T_f s + 1}$$

The state variable x_4 is therefore the capacitor voltage $v_c = v_1 - v_2$ passed through the artificial filter with the constant T_f . The filter is introduced to enable capacitor voltage representation as a state variable, which significantly simplifies modeling, and the time constant is small to computational limits $T_f \approx 0$; therefore it does not introduce new dynamic properties.

The parameters in (14) that depend on α are linearised around the operating point. For the linearisation purpose, the steady-state values for the states $x_1 - x_4$ are obtained in the initialization process using the steady-state modeling in [1-2]. The model linearisation in Q-Q frame follows the methodology given in [6].

4.3 Controller model

The TCSC controller model consists of a second order feedback filter, PI controller, Phase Locked Loop (PLL), series compensator and a transport delay model, as shown in Figure 6. The PLL system is of the $d-q-z$ type and its functional diagram is given in [9-10]. The state-space linearised second-order PLL model is developed in [11]. The PLL synchronises thyristor firings with the line current phase angle.

For simplicity reasons, the TCSC voltage feedback control is used, where V_{ref} can be a function of other parameters at higher control levels. Presently, the research is in progress to develop more advanced control strategy for SSR damping. Because of the thyristor firings at discrete time instants the system is actually a sampled data system with the sampling frequency $f_s = 360 \text{ Hz}$ [6],[11]. The continuous model therefore includes a first order delay, given by time constant T_{dl} , to accommodate the phase lag introduced by sampling the firing angle signal as it is discussed in [7],[12].

The filter time constant is of the order of 2 ms , which is in line with studies in [6],[11]. It should be noted that the voltage phase angle also affects the firing angle because the actual firing angle is measured with respect to the voltage curve. Here, we have direct correlation across each phase, and the sampling frequency is $1/3$ of

f_s and therefore an additional lag is introduced represented by the delay filter with T_{d2} . Simulation results demonstrate improvement in the response with the introduction of this delay element. The second order filter with v_c reduces the harmonics on the feedback signal.

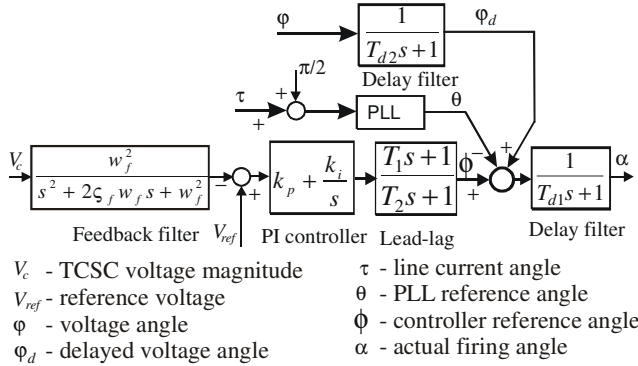


Figure 6: The controller model and firing angle calculation.

4.4 Combined System model

The final model is obtained by connecting the three independent state-space models: 1) generator with mechanical system, 2) AC system with TCSC, and 3) TCSC controller with PLL model.

The three subsystem models are connected using the input and output matrices as presented in [6] and [7]. Such model connection enables flexibility for future studies.

5 SUBSYNCHRONOUS RESONANCE ANALYSIS

Eigenvalue analysis is carried out for the IEEE first benchmark model for SSR studies [7]. This system is characterized by four unstable torsional modes that are distributed in a relatively wide frequency range. A steady-state operating point is chosen in which the machine operates with a power factor of 1 while delivering a power of 0.9 per unit. Self damping of 0.1 is added to the masses in the shaft system. No mutual damping is assumed. Constant field voltage is also assumed. Infinite bus voltage is 477.7 kV. Compensation level is fixed at 40 percent. The remaining data are given the Appendix.

The location of dominant eigenvalues for the above system (compensation with fixed capacitors) is given by “crosses in Figure 7. It is seen that the complex pair “A” is unstable and the frequency of this mode 33Hz indicating the subsynchronous resonance.

The SSR studies on systems with TCSC have been traditionally performed with digital simulation because of the difficulties in analytical modeling of TCSC in wider frequency domain. The developed analytical TCSC model is used here to study eigenvalue location and proximity to subsynchronous resonance on the IEEE benchmark system when compensated with TCSC.

The TCSC parameters are adjusted in such way that with the nominal operating point (at 78deg) the compensation level is identical as in the original subsystem. The TCSC control system is based on relatively simple AC voltage feedback as shown in Figure 6. The location of eigenvalues is shown by “diamonds” in Figure 7. We conclude that the system with TCSC is stable. TCSC improves damping of the mode A but also it improves dynamics at lower frequencies as shown by the complex pair “C”. However TCSC deteriorates damping of mode C which implies that more complex TCSC control solutions should be developed.

The results of the above eigenvalue analysis are validated through PSCAD/EMTDC simulation, as shown in Figure 8. The figure presents the rotor torque components between the masses 3-4 (LPA-LPB) and masses 5-6 (GEN-EXC), which are most sensitive to the subsynchronous instability. At 5 sec, the compensation level is changed by 5% in both systems and it is evident that the system with fixed capacitors is unstable. The system with TCSC is stable as predicted by the eigenvalue study.

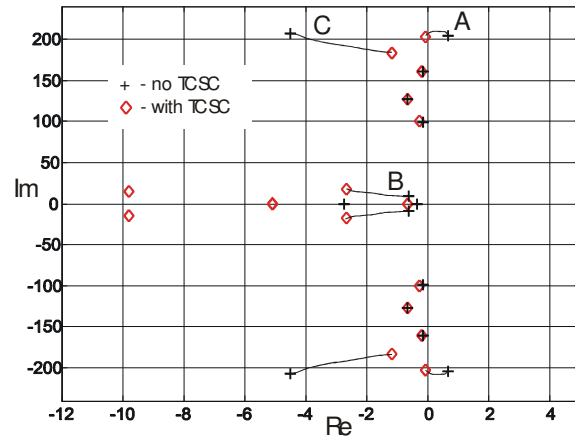


Figure 7: Movement of eigenvalues with the connection of TCSC.

6 CONCLUSIONS

In this paper a simplified linear-continuous model of TCSC is derived using identification methods with frequency response of the non-linear segment. The model includes detailed controller and PLL and it is linked with a linearized model of IEEE SSR benchmark system. The model enables eigenvalue studies at subsynchronous frequencies. It is used to calculate the small signal damping of the subsynchronous modes and the analysis shows improvement in damping if compensation with TCSC is used. Nonlinear simulation studies using PSCAD/EMTDC package validated the results of eigenvalue analysis.

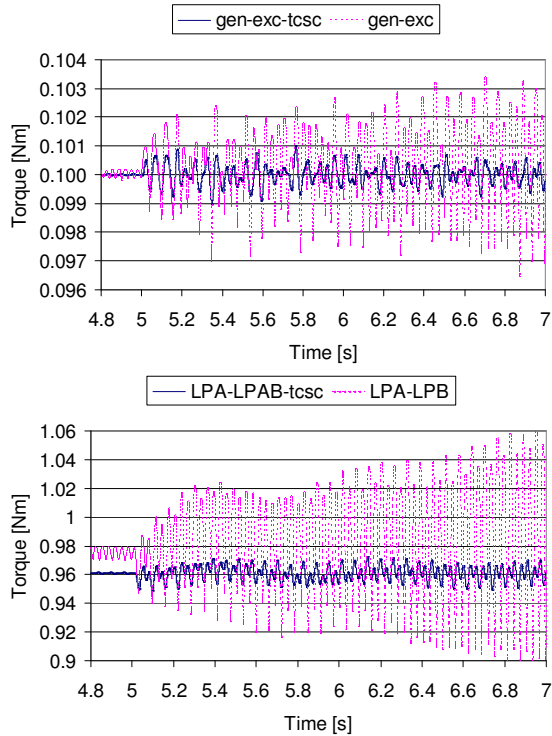


Figure 8: Response of two torque components on the rotor shaft after a 5% step increase in the compensation level.

7 APPENDIX

TCSC data (at nominal point)	
c	$42 \mu F$
l_{cr}	$0.043 H$
V_c	$70.2 kV$
Fir. angl. α	78°
TCSC Controller data	
k_p	$-0.008 rad/kV$
K_I	$-.17 rad/(kVs)$
T_{d1}	$1/220s$
T_{d2}	$1/1400s$
ζ_f	0.9
ω_f	$50 Hz$
PLL k_p	20
T_1	$0.03 s$
T_2	$0.0095 s$

Table 1: TCSC and TCSC controller data.

REFERENCES

- [1] S.G.Jalali, R.A.Hedin, M. Pereira, K.Sadek, "A stability model for the advanced series compensator (ASC)," IEEE Trans. On Power Delivery, Vol 11, No 2, April, 1996. pp 1128-1137
- [2] C.R. Fuerte-Esquivel, E.Acha, H. Ambriz-Perez, "A thyristor controlled series compensator model for the power flow solution of practical power networks," IEEE Trans. On Power Systems, Vol 9, No 15, Feb. 2000. pp 58-64
- [3] S.G.Jalali, R.H.Lasseter I.Dobson, "Dynamic Response of a Thyristor Controlled Switched capacitor" IEEE Trans. On Power Delivery, Vol 9, No 3, July 1994. pp 1609-1615
- [4] A. Ghosh, G.Ledwich, "Modelling and control of thyristor controlled series compensators" IEE Proc. Generation Transmission and Distribution, Vol. 142, No 3, May 1995. pp 297-304
- [5] Mattavelli P, Verghese GC, Stankovic AM, "Phasor Dynamics of Thyristor Controlled Series Capacitor Systems" IEEE Transactions on Power Systems, Vol.12, No.3, Aug. 1997, pp.1259-67
- [6] D. Jovcic, N.Pahalawaththa, M.Zavahir, H.Hassan "SVC dynamic analytical model" IEEE Transactions on Power Delivery, Vol 18, no4, October 2003, pp 1455-1461
- [7] IEEE SSR Task Force, "First benchmark model for computer simulation for subsynchronous resonance," IEEE Transactions on Power Apparatus and Systems, Vol. PAS-96, No.5, Sep/Oct 1977, pp 1565-1571
- [8] K. R. Padiyar, 'Power System Dynamics: Stability and Control', Interline, Bangalore, 1996
- [9] A. Gole, V.K. Sood, L. Mootosamy, "Validation and Analysis of a Grid Control System Using D-Q-Z Transformation for Static compensator Systems", Canadian Conference on Electrical and Computer Engineering Montreal, PQ, Canada September 1989, pp 745-748
- [10] D.Jovcic "Control of High Voltage DC and Flexible AC Transmission Systems", Ph.D. Thesis, University of Auckland, Auckland, New Zealand, 1999
- [11] D.Jovcic, G.N Pillai "Discrete system model of a six-pulse SVC" IASTED EuroPES 2003, Marbella, September 2003, conference proceedings pp 318-323